Understanding of QCD at high density from Z_3-symmetric QCD-like theory

Hiroaki Kouno,[1,*] Kouji Kashiwa,[2,†] Junichi Takahashi,[3,‡] Tatsuhiro Misumi,[4,5,§] and Masanobu Yahiro[3,¶]

[1]*Department of Physics, Saga University, Saga 840-8502, Japan*
[2]*Yukawa Institute for Theoretical Physics, Kyoto University, Kyoto 606-8502, Japan*
[3]*Department of Physics, Graduate School of Sciences, Kyushu University, Fukuoka 812-8581, Japan*
[4]*Department of Physics, Keio University, Hiyoshi 4-1-1,Yokohama, Kanagawa 223-8521, Japan*
[5]*Department of Mathematical science, Akita University, 1-1 Tegata Gakuen-machi, Akita 010-8502, Japan*

(Dated: March 4, 2022)

We investigate QCD at large μ/T by using Z_3-symmetric $SU(3)$ gauge theory, where μ is the quark-number chemical potential and T is temperature. We impose the flavor-dependent twist boundary condition on quarks in QCD. This QCD-like theory has the twist angle θ as a parameter, and agrees with QCD when $\theta = 0$ and becomes symmetric when $\theta = 2\pi/3$. For both QCD and the Z_3-symmetric $SU(3)$ gauge theory, the phase diagram is drawn in μ–T plane with the Polyakov-loop extended Nambu–Jona-Lasinio model. In the Z_3-symmetric $SU(3)$ gauge theory, the Polyakov loop φ is zero in the confined phase appearing at $T \lesssim 200$ MeV. The perfectly confined phase never coexists with the color superconducting (CSC) phase, since finite diquark condensate in the CSC phase breaks Z_3 symmetry and then makes φ finite. When $\mu \gtrsim 300$ MeV, the CSC phase is more stable than the perfectly confined phase at $T \lesssim 100$ MeV. Meanwhile, the chiral symmetry can be broken in the perfectly confined phase, since the chiral condensate is Z_3 invariant. Consequently, the perfectly confined phase is divided into the perfectly confined phase without chiral symmetry restoration in a region of $\mu \lesssim 300$ MeV and $T \lesssim 200$ MeV and the perfectly confined phase with chiral symmetry restoration in a region of $\mu \gtrsim 300$ MeV and $100 \lesssim T \lesssim 200$ MeV. The basic phase structure of Z_3-symmetric QCD-like theory remains in QCD. We show that in the perfectly confined phase the sign problem becomes less serious because of $\varphi = 0$, using the heavy quark theory. We discuss a lattice QCD framework to evaluate observables at $\theta = 0$ from those at $\theta = 2\pi/3$.

PACS numbers: 11.30.Rd, 12.40.-y

arXiv:1504.07585v1 [hep-ph] 28 Apr 2015

I. INTRODUCTION

Quantum chromodynamics (QCD) has a lot of interesting phenomena particularly at small temperature (T) and large quark-number chemical potential (μ). The phenomena may affect the structure of neutron stars in its inner core. The color superconducting (CSC) phase that appears only at large μ/T is a typical example. However, lattice QCD (LQCD) simulations as the first-principle calculation have the well-known sign problem, since the fermion determinant becomes complex for real μ and this makes the importance-sampling method unfeasible in Monte Carlo simulations. Therefore, several methods such as the reweighting method [1], the Taylor expansion method [2, 3] and the analytic continuation from imaginary to real μ [4–9] were proposed so far to circumvent this problem, but these methods are considered to be reliable only at $\mu/T \lesssim 1$. Recently, remarkable progress has been made with the complex Langevin dynamics [10–14] and the Lefschetz thimbles approach [15, 16]. However, the results are still far from perfection. Hence the effective model approach becomes useful. Actually, QCD at large μ/T has been predicted with effective models such as the Polyakov loop extended Nambu-Jona-Lasinio (PNJL) model [17–29].

The LQCD and effective model approaches have a fundamental problem on the definition of quark confinement, as mentioned below. It is widely believed that the confinement mechanism in $SU(N)$ gauge theory is governed by Z_N symmetry and confinement and deconfinement phases are defined by the Polyakov loop φ [30] as an order parameter for Z_N symmetry. This is true for pure gauge theory, since Z_N symmetry is exact. The symmetry is preserved at small T, but spontaneously broken at high T. This makes the confinement-deconfinement transition first-order in the case of $N \geq 3$. In $SU(N)$ gauge theory with fundamental fermions, Z_N symmetry is not exact any more, so that the definition of confinement and deconfinement phases becomes obscure. In fact, in QCD with $N = 3$, φ is always finite at $T > 0$ and the deconfinement transition is crossover for zero μ [31].

An attempt to answer this problem was made recently by modifying the fermion boundary condition in Refs. [32–35]. Three degenerate flavor QCD was extended by imposing the flavor-dependent twist boundary condition (FTBC)

$$\Psi_f(\tau = \beta, \mathbf{x}) = -e^{-i\theta_f}\Psi_f(\tau = 0, \mathbf{x}) \tag{1}$$

on quarks, where $\beta = 1/T$ and Ψ_f is the quark field with flavor f. When the twist angles θ_f are set to

$$\theta_1 = \theta, \quad \theta_2 = -\theta, \quad \theta_3 = 0, \tag{2}$$

the QCD-like theory agrees with QCD when $\theta = 0$, and becomes Z_3 symmetric when $\theta = 2\pi/3$, since θ_f is transformed into θ_{f-1} by the Z_3 transformation but θ_{f-1} returns to θ_f by relabeling f. The Z_3-symmetric QCD-like theory with $\theta = 2\pi/3$ is referred to as Z_3-QCD in this paper.

*kounoh@cc.saga-u.ac.jp
†kouji.kashiwa@yukawa.kyoto-u.ac.jp
‡takahashi@phys.kyushu-u.ac.jp
§misumi@phys-h.keio.ac.jp
¶yahiro@phys.kyushu-u.ac.jp

Confinement and deconfinement phases are clearly defined with φ in Z_3-QCD. The QCD phase diagram can be understood as a remnant of the Z_3-QCD phase diagram. In Z_3-QCD, it is obvious that there exists a confinement phase at small T and a deconfinement phase at high T, because $\varphi = 0$ in the low-T limit and 1 in the high-T limit. We call the phase where $\varphi = 0$ perfectly confined phase in this paper. The deconfinement phase transition is either first-order or second-order. The order of the phase transition was investigated by applying the FTBC to the PNJL model, and was found to be first-order at $\mu = 0$ [32–35]. LQCD simulations for 2+1 flavor quarks show that φ is quite small at zero μ and low T [36, 37]. The confinement property in 2+1 flavor QCD is considered to be a remnant of the perfectly confined phase in Z_3-QCD.

Z_3-QCD is useful also to investigate the relation between confinement and other mechanism such as chiral symmetry breaking and CSC. Particularly for the relation between confinement and CSC, we can make clear discussion by using Z_3 symmetry. The diquark condensate Δ as an order parameter for CSC is not Z_3 invariant. This means that Δ is an order parameter for both CSC and Z_3 symmetry. The diquark condensate is then zero whenever φ is zero, and hence the CSC phase with finite Δ never coexists with the perfectly confined phase with zero φ. The correlation between φ and the diquark condensate is thus clearly understood in Z_3-QCD. The correlation in QCD can be understood as a remnant of that in Z_3-QCD. Meanwhile, the chiral condensate as an order parameter for chiral symmetry is Z_3 invariant. Hence, a chiral transition can take place in the perfectly confined phase. In fact, the PNJL model shows that this really happens at finite μ [33]. In the PNJL analysis, however, diquark effects were not considered.

In this paper, we try to understand QCD at high μ/T from Z_3-QCD. The phase diagram is drawn in μ–T plane for both QCD and Z_3-QCD by using the PNJL model with the FTBC. In the case of Z_3-QCD, a perfectly confined phase with $\varphi = 0$ and $\Delta = 0$ appears at $T \lesssim 200$ MeV, and the chiral restoration occurs at $\mu \approx 300$ MeV in the phase, as expected. Hence, the perfectly confined phase is divided into the perfectly confined phase without chiral symmetry restoration in a region of $\mu \lesssim 300$ MeV and $T \lesssim 200$ MeV and the perfectly confined phase with chiral symmetry restoration in a region of $\mu \gtrsim 300$ MeV and $100 \lesssim T \lesssim 200$ MeV. In a region of $\mu \gtrsim 300$ MeV and $T \lesssim 100$ MeV, CSC phases with finite Δ and small φ come out, since they cannot coexist with the perfectly confined phase and more stable than the perfectly confined phase with chiral symmetry restoration. This basic structure remains in QCD. Second we show that in the perfectly confined phase the sign problem may become less serious because of $\varphi = 0$, using the heavy quark model. This may make LQCD simulations feasible in the perfectly confined phase. Particularly when the system is in the perfectly confined phase without chiral symmetry restoration, the system changes continuously from Z_3-QCD to QCD by varying θ from $2\pi/3$ to 0. Using this property, we propose a way of estimating observables for QCD from those for Z_3-QCD.

This paper is organized as follows. We recapitulate the FTBC and Z_3-QCD in Sec. II and the PNJL model in Sec. III. Numerical results are shown by using the PNJL model and LQCD simulations in Sec. IV. The sign problem in Z_3-QCD is discussed in Sec. V. Section VI is devoted to a summary.

II. Z_3-QCD

In this section, we recapitulate the FTBC and Z_3-QCD, following Refs. [32–35]. We consider $SU(N)$ gauge theory with N degenerate flavor quarks. The Lagrangian density $\mathcal{L}$ in Euclidean spacetime is

$$\mathcal{L} = \sum_{f=1}^{N} \bar{\Psi}_f(\gamma_\nu D_\nu + m)\Psi_f + \frac{1}{4g^2} F_{\mu\nu}^{a\ 2}, \tag{3}$$

where m is the current quark mass for all flavors and $D_\nu \equiv \partial_\nu - iA_\nu$ for the gauge field A_μ and $F_{\mu\nu}$ is the field strength tensor. The temporal boundary conditions for quarks are

$$\Psi_f(\tau = \beta, \mathbf{x}) = -\Psi_f(\tau = 0, \mathbf{x}). \tag{4}$$

The Lagrangian density (3) is invariant under the Z_N (large gauge) transformation,

$$\begin{aligned} \Psi_f &\rightarrow \Psi'_f = U\Psi_f, \\ A_\nu &\rightarrow A'_\nu = UA_\nu U^{-1} + i(\partial_\nu U)U^{-1}, \end{aligned} \tag{5}$$

but the boundary condition (4) is changed into [38]

$$\Psi_f(\tau = \beta, \mathbf{x}) = -e^{i2k\pi/N}\Psi_f(\tau = 0, \mathbf{x}). \tag{6}$$

Here

$$U(x, \tau) = \exp(i\alpha_a t_a) \tag{7}$$

is an element of $SU(N)$ group characterized by real functions $\alpha_a(x, \tau)$ satisfying the boundary condition

$$U(x, \beta) = \exp(-i2\pi k/N)U(x, 0) \tag{8}$$

for any integer k.

Now, we consider the following FTBC instead of (4):

$$\Psi_f(\tau = \beta, \mathbf{x}) = -e^{-i\theta_f}\Psi_f(\tau = 0, \mathbf{x}), \tag{9}$$

where

$$\theta_f = \theta_1 + \frac{2\pi}{N_f}(f-1) \quad (f = 1, 2, \ldots, N_f), \tag{10}$$

with $N_f = N$. Under the Z_N transformation (5), the boundary condition (9) is changed into

$$\Psi_f(\tau = \beta, \mathbf{x}) = -e^{-i\theta'_f}\Psi_f(\tau = 0, \mathbf{x}), \tag{11}$$

where

$$\theta'_f = \theta_1 + \frac{2\pi}{N}(f-1-k) \quad (f = 1, 2, \ldots, N). \tag{12}$$

The boundary condition (12) returns to the original one (10) by relabeling the flavor index $f-k$ as f. Hence $SU(N)$ gauge

theory with the FTBC (9) has Z_N symmetry exactly. $SU(N)$ gauge theory with $l \times N$ flavor fundamental quarks also has Z_N symmetry for any positive integer l, when the FTBC (9) with $N_f = lN$ is imposed on the fermions [32].

When the fermion fields Ψ_f are transformed as [38]

$$\Psi_f \to \exp\left(-i\theta_f T\tau\right)\Psi_f, \tag{13}$$

the boundary condition (9) returns to the ordinary one (4), but the Lagrangian density $\mathcal{L}$ is changed into

$$\mathcal{L}^\theta = \sum_{f=1}^{N} \bar{\Psi}_f(\gamma_\nu D_\nu^\theta + m)\Psi_f + \frac{1}{4g^2}{F_{\mu\nu}^a}^2, \tag{14}$$

where $D_\nu^\theta \equiv \partial_\nu - i(A_\nu + \hat{\theta}\delta_{\nu,4}T)$ and $i\hat{\theta}T$ is the flavor-dependent imaginary chemical potential given by the matrix

$$\begin{aligned}\hat{\theta} &= \mathrm{diag}(\theta_1, \theta_2, \cdots, \theta_N) \\ &= \mathrm{diag}(\theta_1, \theta_1 + 2\pi/N, \cdots, \\ &\quad \theta_1 + 2(f-1)\pi/N, \cdots, \theta_1 + 2\pi(N-1)/N)\end{aligned} \tag{15}$$

in flavor space. In the case of $N = 3$, $\mathcal{L}^\theta$ is nothing but the Lagrangian density of Z_3-QCD. The flavor-dependent imaginary chemical potential breaks $SU(N)$ flavor symmetry and associated $SU(N)$ chiral symmetry [32, 33]. In the chiral limit, global $SU_{\rm V}(3) \times SU_{\rm A}(3)$ symmetry is broken down to $(U(1)_{\rm V})^2 \otimes (U(1)_{\rm A})^2$ [34]. The symmetry is even broken into $(U(1)_{\rm V})^2$, when chiral symmetry is spontaneously violated.

III. PNJL MODEL WITH FLAVOR-DEPENDENT TWIST BOUNDARY CONDITION

In this section, we explain the Polyakov-loop extended Nambu-Jona-Lasinio (PNJL) model with the FTBC (9) and diquark effects. Taking the Polyakov-gauge and treating A_4 as a background gauge field, one can get the model Lagrangian density for three degenerate flavors as

$$\mathcal{L}^\theta_{\rm PNJL} = \sum_{f=u,d,s} \bar{\Psi}_f(\gamma_\nu D_\nu^\theta + m)\Psi_f + \mathcal{L}^{\rm int}_{\rm NJL} + \mathcal{U}, \tag{16}$$

where $D_\nu^\theta = \partial_\nu - i\delta_{\nu,4}(A_4 + \hat{\theta}T)$. In (16), $\mathcal{U}$ is a function of φ and its complex conjugate φ^* defined by

$$\begin{aligned}\varphi &= \frac{1}{3}\mathrm{tr}_c[e^{iA_4/T}] \\ &= \frac{1}{3}(e^{i\phi_1} + e^{i\phi_2} + e^{i\phi_3}),\end{aligned} \tag{17}$$

with the condition $\phi_1 + \phi_2 + \phi_3 = 0$.

We take the following form [22] as $\mathcal{U}$:

$$\begin{aligned}\mathcal{U} = T^4\Big[&-\frac{a(T)}{2}\varphi^*\varphi \\ &+ b(T)\ln(1 - 6\varphi\varphi^* + 4(\varphi^3 + {\varphi^*}^3) - 3(\varphi\varphi^*)^2)\Big],\end{aligned} \tag{18}$$

$$a(T) = a_0 + a_1\Big(\frac{T_0}{T}\Big) + a_2\Big(\frac{T_0}{T}\Big)^2, \quad b(T) = b_3\Big(\frac{T_0}{T}\Big)^3. \tag{19}$$

The parameters in $\mathcal{U}$ are determined from LQCD data [39, 40] in the pure gauge (heavy quark) limit. The Polyakov-loop potential has a first-order deconfinement phase transition at $T = T_0$ in the limit, and hence $T_0 = 270$ MeV. In the case of finite quark mass, however, the PNJL model with this value overestimates the pseudocritical temperature $T_c \approx 160$ MeV at zero μ determined by full LQCD [41–43]. We have then rescaled T_0 to 195 MeV to reproduce $T_c \sim 160$ MeV [29]. The parameters in the Polyakov-loop potential are summarized in Table I(a).

(a)	a_0	a_1	a_2	b_3	T_0(MeV)
	3.51	-2.47	15.2	-1.75	195
(b)	m_f(MeV)	Λ(MeV)	$G_{\rm S}\Lambda^2$	$G_{\rm D}\Lambda^2$	$K\Lambda^5$
	5.5	602.3	1.835	$\frac{3}{4}G_{\rm S}\Lambda^2$	12.36

TABLE I: Summary of the parameter set in the PNJL model for the case of $N = 3$. Panels (a) and (b) show the parameters in the Polyakov-loop potential and the NJL sector, respectively.

In (16), $\mathcal{L}^{\rm int}_{\rm NJL}$ stands for the effective quark-antiquark and quark-quark interactions [44]:

$$\begin{aligned}\mathcal{L}^{\rm int}_{\rm NJL} &= -G_{\rm S}\sum_{a=0}^{8}[(\bar{\Psi}\lambda_a\Psi)^2 + (\bar{\Psi}i\gamma_5\lambda_a\Psi)^2] \\ &\quad -G_{\rm D}\sum_{\alpha=u,d,s}^{4}\sum_{c=r,g,b}[(\bar{\Psi})^a_\alpha i\gamma_5\epsilon^{\alpha\beta\gamma}\epsilon_{abc}(\Psi_C)^b_\beta] \\ &\quad \times[(\bar{\Psi}_C)^u_\rho i\gamma_5\epsilon^{\rho\sigma\gamma}\epsilon_{uvc}(\Psi)^v_\sigma] \\ &\quad +K\left[\det_{ff'}\bar{\Psi}_f(1+\gamma_5)\Psi_{f'} + \mathrm{h.c.}\right],\end{aligned} \tag{20}$$

where the λ_a are the Gell-Mann matrices in flavor space, $G_{\rm S}$ and G_D are coupling constants of the four-quark interactions and K is a coupling constant of the Kobayashi-Maskawa-'t Hooft determinant interaction [45, 46]. The quark field Ψ^a_α carries color ($a = r, g, b$) and flavor ($\alpha = u, d, s$) indices. The values of coupling constants, current quark mass and three dimensional momentum cutoff Λ are tabulated in Table I(b). The coupling constants and the cutoff were determined to reproduce empirical values of η'- and π-meson masses and π-meson decay constant at vacuum when $m_u = m_d = 5.5$MeV and $m_s = 140.7$MeV [47]. In this paper, however, we consider a symmetric current quark mass of $m = m_f = 5.5$ MeV to preserve SU(3) flavor symmetry.

Taking the mean field approximation, one can get the thermodynamic potential per volume as

$$\begin{aligned}\Omega &= \Omega_q + U + \mathcal{U} \\ &\quad -\sum_{j=1}^{2NN_f}\int\frac{d^3p}{(2\pi)^3}\Big[E_j + \frac{2}{\beta}\ln\left(1 + e^{-\beta E_j}\right)\Big],\end{aligned} \tag{21}$$

where the mean-field potential part U is given by

$$\begin{aligned}U &= G_{\rm D}\sum_{l=1,2,3}|\tilde{\Delta}_l|^2 + 2G_{\rm S}\sum_{f=u,d,s}\sigma_f^2 \\ &\quad -4K\sigma_u\sigma_d\sigma_s\end{aligned} \tag{22}$$

with chiral condensates $\sigma_f = \langle\bar{\Psi}_f\Psi_f\rangle$ for $f = u, d, s$ and diquark condensates $\tilde{\Delta}_l = \langle(\bar{\Psi}_C)^a_\alpha i\gamma_5\epsilon^{\alpha\beta l}\epsilon_{abl}\Psi^b_\beta\rangle$ where no sum is taken over l on the right hand side. In (22), the E_j are the quark spectra which depend on the absolute value of three-dimensional quark momentum $\mathbf{p}$, the effective quark mass

$$M_f = m_f - 4G_{\rm S}\sigma_f + 2K\sigma_{f'}\sigma_{f''}, \quad (f \neq f',\ f \neq f'',\ f' \neq f'') \tag{23}$$

the diquark condensate (multiplied by $-2G_{\rm D}$)

$$\Delta_l = -2G_{\rm D}\tilde{\Delta}_l, \tag{24}$$

and the effective chemical potential

$$\mu^c_f = \mu + i\phi_c T + i\theta_f T. \tag{25}$$

It is difficult to obtain the explicit forms of E_j analytically, but we can determine the E_j by solving the eigenvalue equation for Dirac operator numerically. Using these spectra, we can calculate Ω and then find the solutions σ_f, Δ_l and φ that minimize Ω. Obviously, σ_f is invariant under the Z_3 transformation (5), but Δ_l is not.

IV. NUMERICAL RESULTS

In this section, we show numerical results of the PNJL model. For later convenience, we put

$$\theta_u = \theta_1 = \theta, \quad \theta_d = \theta_2 = -\theta, \quad \theta_s = \theta_3 = 0. \tag{26}$$

The fermion boundary condition (26) agrees with the FTBC (10) when $\theta = 2\pi/3$ and the standard antiperiodic boundary condition when $\theta = 0$.

In Z_3-QCD with $\theta = 2\pi/3$, the flavor symmetry is violated with the FTBC (as the mentioned above about the flavor-dependent imaginary chemical potential), but u and d quarks are symmetric under the interchange between u and d. Since the boundary condition is changed by the Z_3 gauge transformation, flavor and diquark indices are renamed so that the conditions $M_1 \leq M_2 \leq M_3$ and $|\Delta_1| \leq |\Delta_2| \leq |\Delta_3|$ can be satisfied.

Figure 1 shows T dependence of the absolute value of diquark condensates Δ_1, Δ_2 and Δ_3 at $\mu = 340$ MeV for Z_3-QCD with $\theta = 2\pi/3$. There appear a variety of CSC phases [44]. Below $T = T_1 = 10$ MeV, all the diquark condensates are finite, indicating that it is the color flavor locking (CFL) phase. Two of three condensates are finite in the region $T_1 \leq T \leq T_2 = 80$ MeV, and one of three is finite in the region $T_3 = 223 \leq T \leq T_4 = 419$ MeV. This means that the former is the uSC phase and the latter is the 2SC phase.

In Fig. 2, the average values of dynamical quark masses and the absolute value of diquark condensates, namely, $M = (M_1+M_2+M_3)/3$ and $\Delta = (|\Delta_1|+|\Delta_2|+|\Delta_3|)/3$, are plotted as a function of T, together with $\Phi \equiv |\varphi|$, at $\mu = 340$ MeV for Z_3-QCD with $\theta = 2\pi/3$. There are three equivalent solutions to φ: $\varphi = \Phi e^{i\phi}$ with $\phi = 0, \pm 2\pi/3$ (or $\phi = \pi, \pm\pi/3$). The solutions of $\phi = \pm 2\pi/3$ $(\pm\pi/3)$ are Z_3 images of the solution of $\phi = 0$ (π). In fact, they are thermodynamically equivalent and are transformed from one to another by the Z_3 transformation. We can then take the solution of $\phi = 0$ (π), and φ is real. As mentioned in Sec. I, finite diquark condensates in CSC phases break Z_3 symmetry and hence induce finite Φ. In the CFL and uSC phases below T_2, Φ is tiny but finite, as expected. Thus, CSC phases do not coexist with the perfectly confined phase, but with the almost-confined phase. Also in the 2SC phase at $T_3 < T < T_4$, Φ is finite as expected, but it is large. Thus quarks are deconfined in the 2SC phase. In the region $T_2 < T < T_3$, Φ is zero and hence diquark condensates are also zero. This is the perfectly confined phase. Above T_4, Φ is finite but Δ is zero. This is the pure deconfinement phase without diquark condensate.

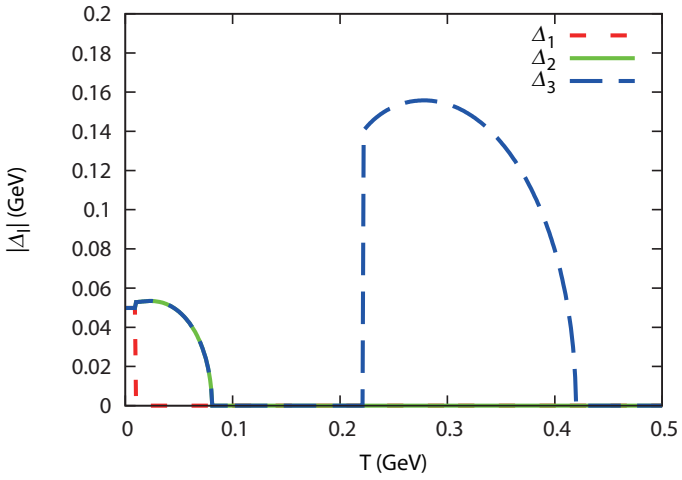


Fig. 1: T dependence of $|\Delta_l|$ at $\mu = 340$ MeV in the PNJL model with $\theta = 2\pi/3$. The diquark condensates Δ_1, Δ_2 and Δ_3 are denoted by dashed, solid and long dashed lines, respectively. Below $T = 10$ MeV, three diquark condensates exist. In a region of $T = 10 \sim 80$ MeV, $\Delta_1 = 0$ and $\Delta_2 = \Delta_3$.

Figure 3 is the same as Fig. 1, but for QCD with $\theta = 0$. Below $T = T_1 = 32$ MeV, all Δ_l are finite, indicating that it is the CFL phase. In the region $T_1 \leq T \leq T_2 = 86$ MeV, one of three appears. It is the 2SC phase. The phase structure is thus much simpler at $\theta = 0$ than at $\theta = 2\pi/3$. Figure 4 is the same as Fig. 2, but for $\theta = 0$. In this case, φ is always real and $\varphi = |\varphi| = \Phi$. Since Z_3 symmetry is not exact in this case, Φ is always finite at $T > 0$. Thus we cannot define the confinement and deconfinement phases clearly. Since Φ is small in the CFL and 2SC phases, one can consider that the CSC phases are in the almost-confined phase.

Figure 5 shows the phase diagram in μ–T plane for the case of $\theta = 2\pi/3$. A variety of phases are present in this case. When T increases from zero with μ fixed at a large value, say 350 MeV, the CFL, uSC, perfectly-confined, 2SC and pure deconfinement phases appear. We also see that the chiral transition takes place in the perfectly confined phase.

Figure 6 is the same as Figure 5 but for $\theta = 0$. The uSC phase disappears and the 2SC goes down to lower T, while at small T the CFL phase remains and the perfectly-

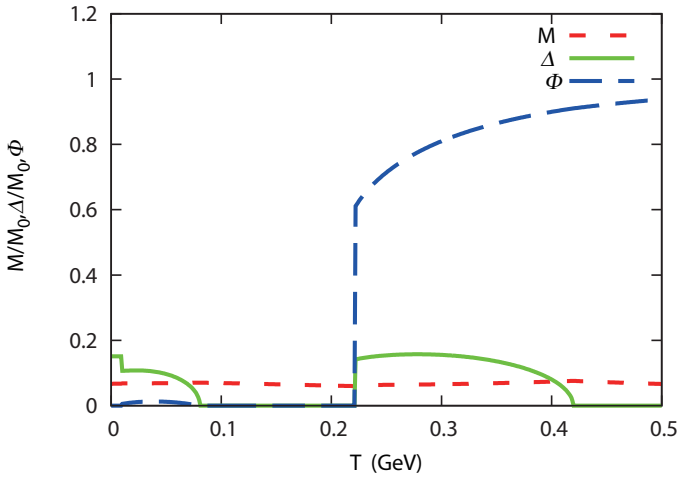


Fig. 2: T dependence of M, Δ, and Φ at $\mu = 340$ MeV in the PNJL model with $\theta = 2\pi/3$. Here, M, Δ and Φ are denoted by dashed, solid and long dashed lines, respectively, and M and Δ are normalized by the constituent quark mass M_0 at the vacuum.

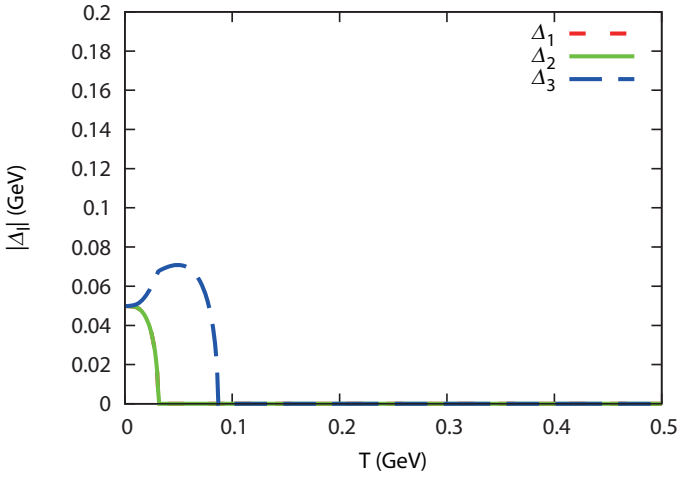


Fig. 3: T dependence of $|\Delta_l|$ at $\mu = 340$ MeV in the PNJL model with $\theta = 0$. See Fig. 1 for the definition of lines.

confined phase becomes an almost-confined phase without diquark condensate. The almost-confined phase and the CFL phase at low T can thus be regarded as remnants of the perfectly confined phase and the CFL phase in Z_3-QCD.

V. SIGN PROBLEM IN Z_3-QCD

It is well known that LQCD has the sign problem at real μ and it makes the importance sampling method unfeasible. Also in the case of Z_3-QCD, the sign problem exists in principle. In fact, the determinant of Dirac operator $\mathcal{M}$ has the

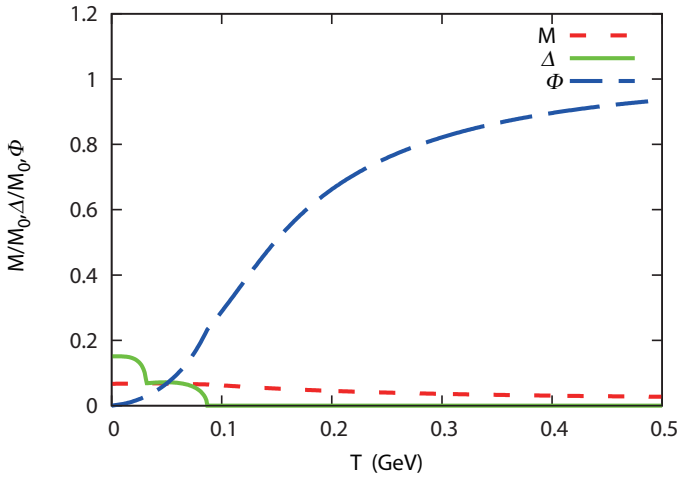


Fig. 4: T dependence of M, Δ and Φ at $\mu = 340$ MeV in the PNJL model with $\theta = 0$. Here M and Δ are divided by M_0. See Fig. 2 for the definition of lines.

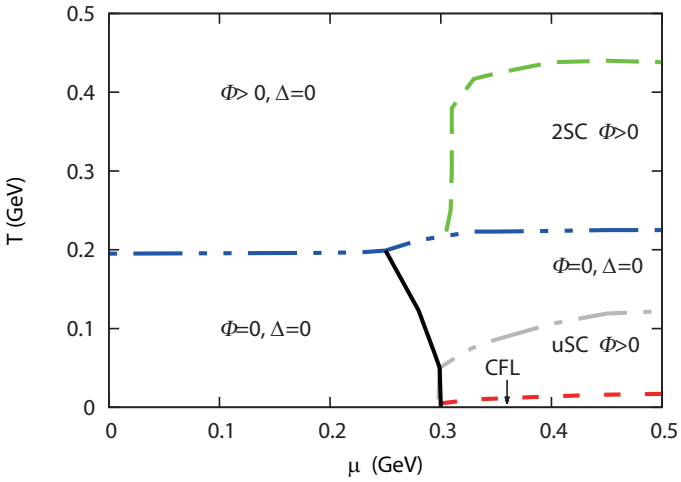


Fig. 5: Phase diagram in the PNJL model with $\theta = 2\pi/3$. The CFL phase exists below the dotted line. The solid line stands for the first-order chiral phase transition; M is large on the left side of the solid line, but small on the right side. The dashed double-dotted line denotes the first-order deconfinement phase transition; the system is in the confinement phase below the line and in the deconfinement phase above the line. The perfectly confined phase is labeled by "$\Phi = 0$, $\Delta = 0$", while the CFL, uSC and 2SC phases are by "CFL","uSC" and "2SC", respectively.

following relation [33]:

$$\begin{aligned}
[\det \mathcal{M}(\mu_f)]^* &= \det \mathcal{M}(-\mu_f^*) \\
&= \prod_{f=u,d,s} \det[D - (\mu - i\theta_f T)\gamma_4 + m_f] \\
&= \prod_{f=u,d,s} \det[D - (\mu + i\theta_f T)\gamma_4 + m_f] \\
&= \det \mathcal{M}(-\mu_f) \qquad (27)
\end{aligned}$$

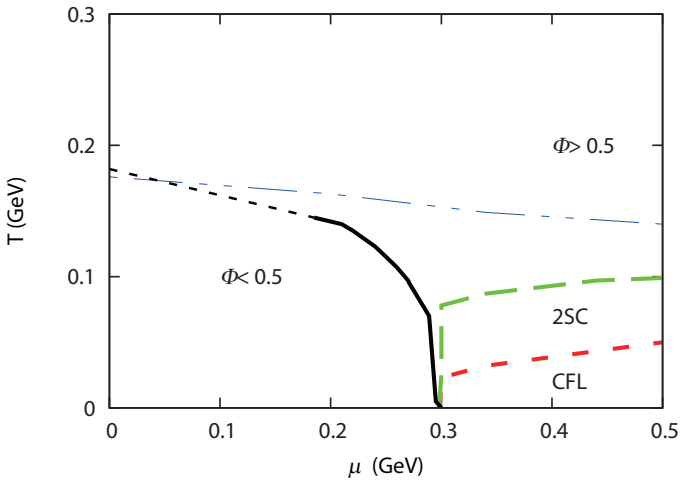


Fig. 6: Phase diagram in the PNJL model with $\theta = 0$. The solid line (thin dotted line) stands for the first-order (crossover) chiral transition. The thin dashed double-dotted line denotes the line of $\Phi = 0.5$. The almost-confined phase is labeled by "$\Phi < 0.5$", while the deconfined phase is by "$\Phi > 0.5$" and the CFL and 2SC phases are by "CFL" and "2SC", respectively.

for $\mu_f = \mu + i\theta_f T$ satisfying the condition (26), where the third equality has been obtained by relabeling the f. Hence, the determinant $\det\mathcal{M}(\mu_f)$ is not real. The present system thus has the sign problem, although the partition function is real, since

$$Z(\mu_f)^* = Z(-\mu_f) = Z(\mu_f), \tag{28}$$

where the first equality comes from (27) and the second one from charge conjugation. Note that Eq. (28) is true for any value of θ.

Although Z_3-QCD has the sign problem at real μ, there is a possibility that it is not serious in the perfectly-confined phase. To see this clearly, we consider the heavy quark model [13, 14]. In the model, the fermion determinant of Dirac operator is given in terms of the Polyakov line operator $\mathrm{Tr}[U_\mathrm{x}]$:

$$\det\mathcal{M}(\mu_f) = \det[1 + he^{\mu/T}U_\mathrm{x}]\det[1 + he^{-\mu/T}U_\mathrm{x}^\dagger] \tag{29}$$

with

$$\begin{aligned}\det[1 + he^{\mu/T}U_\mathrm{x}] &= 1 + he^{\mu/T}\mathrm{Tr}[U_\mathrm{x}] \\ &\quad + h^2e^{2\mu/T}\mathrm{Tr}[U_\mathrm{x}^\dagger] + h^3e^{3\mu/T}, \\ \det[1 + he^{-\mu/T}U_\mathrm{x}^\dagger] &= 1 + he^{-\mu/T}\mathrm{Tr}[U_\mathrm{x}^\dagger] \\ &\quad + h^2e^{-2\mu/T}\mathrm{Tr}[U_\mathrm{x}] + h^3e^{-3\mu/T},\end{aligned} \tag{30}$$

where $U_\mathrm{x} = U(\mathrm{x}, 0)$ for the lattice link variable $U(\mathrm{x}, 0)$ depending on the space coordinate $\mathbf{x}$ only. The parameter h is defined as $h = \zeta^{N_t}$ with the lattice-site number N_t in the temporal direction and the hopping parameter ζ for Wilson fermion and $1/(2m)$ for staggered fermion with a current quark mass m. In general, $\det\mathcal{M}(\mu_f)$ is not real, since the exponential factor with $\mathrm{Tr}[U_\mathrm{x}]$ is not equal to that with its conjugate $\mathrm{Tr}[U_\mathrm{x}]^\dagger$. For the configurations that satisfy the condition $\mathrm{Tr}[U_\mathrm{x}] = 0$, however, only the first and fourth terms remain on the right hand side of of (30), and hence $\det\mathcal{M}(\mu_f)$ becomes real. In Z_3-QCD, we use μ_f instead of μ, but the factor $e^{\pm 3\mu_f/T} = e^{\pm 3\mu}$ is still real when $\theta = 2\pi/3$. This indicates the possibility that the sign problem may not be serious in the perfectly confined phase, since the gauge configurations are concentrated on the vicinity of $\Phi = 0$. One may then perform the importance sampling in lattice Z_3-QCD.

Once a thermodynamical quantity $O(\theta)$ and it derivatives with respect to θ are obtained at $\theta = 2\pi/3$, the quantities at θ less than $2\pi/3$ are obtainable by using the Taylor expansion

$$O(\theta) = \sum_{n=0}^{\infty} \frac{1}{n!} \left.\frac{\partial^n O(\theta)}{\partial\theta^n}\right|_{\theta=2\pi/3} \left(\theta - \frac{2\pi}{3}\right)^n. \tag{31}$$

First we consider the perfectly confined phase with chiral symmetry breaking in Z_3-QCD. The phase is located in a region of $T \lesssim 200$ MeV and $\mu \lesssim 300$ MeV. In QCD with $\theta = 0$, it is very likely that the region includes the nuclear-matter region at $\mu \approx 300$ MeV and $T = 0$.

Figure 7 shows θ dependence of Φ and the quark number density n_q at the point $(\mu, T) = (260\ \mathrm{MeV}, 100\ \mathrm{MeV})$. At $\theta = 2\pi/3$, this point is in the perfectly confined phase with chiral symmetry breaking. We see that the θ-dependence is smooth in a range of $\theta = 0 \sim 2\pi/3$. Hence, the approach mentioned above may be valid for this point because there is no singularity. In particular, Φ increases monotonically as θ decreases from $\theta = 2\pi/3$. This may suggest that only the lower derivative terms are needed in the Taylor expansion (31) to evaluate Φ at smaller θ. On the contrary, n_q has a minimum at $\theta \sim 1.3$. In the Stefan-Boltzmann limit, n_q is given by

$$\begin{aligned} n_q &= (\mu + i\theta T)T^2 + (\mu + i\theta T)^3 \\ &\quad + (\mu - i\theta T)T^2 + (\mu - i\theta T)^3 \\ &= 2\left(\mu T^2 + \mu^3 - 3\mu\theta^2 T^2\right), \end{aligned} \tag{32}$$

and it decreases monotonically as θ increases from $\theta = 0$. As easily seen in Eq. (30), however, the θ term is suppressed by strong confinement near $\theta = 2\pi/3$. As a consequence of the suppression, n_q is considered to have a minimum at $\theta \sim 1.3$. The fact that θ dependence is not monotonic for n_q means that the higher derivative terms are necessary in (31) to evaluate n_q at smaller θ.

Figure 8 is the same as Fig. 7 but at the point $(\mu, T) = (300\ \mathrm{MeV}, 100\ \mathrm{MeV})$. At $\theta = 2\pi/3$, this point is in the perfectly confined phase with chiral symmetry restoration. We see that both Φ and n_q have discontinuities as a function of θ. Hence, the Taylor-expansion approach of (31) does not work at this point. Thus, the Taylor-expansion approach of (31) may work, if the system is in the perfectly confined phase with chiral symmetry breaking in the case of Z_3-QCD.

We remark that, in the numerical calculations for Figs. 7 and 8, we assumed that the diquark condensate does not appear in the whole region of $\theta = 0 \sim 2\pi/3$. Since the analytic

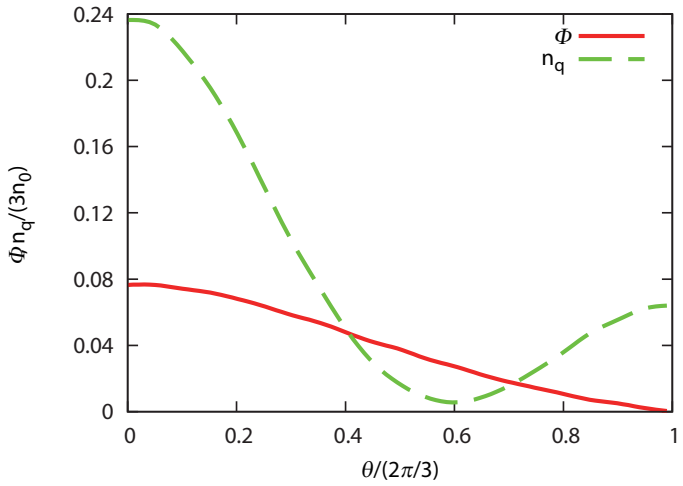


Fig. 7: θ dependence of Φ and the quark number density n_q at $(\mu, T) = (260\ \mathrm{MeV}, 100\ \mathrm{MeV})$ in the PNJL model. The solid line stands for Φ, while the dashed line corresponds to n_q. The n_q is divided by $3n_0$, where n_0 is the normal nuclear matter density.

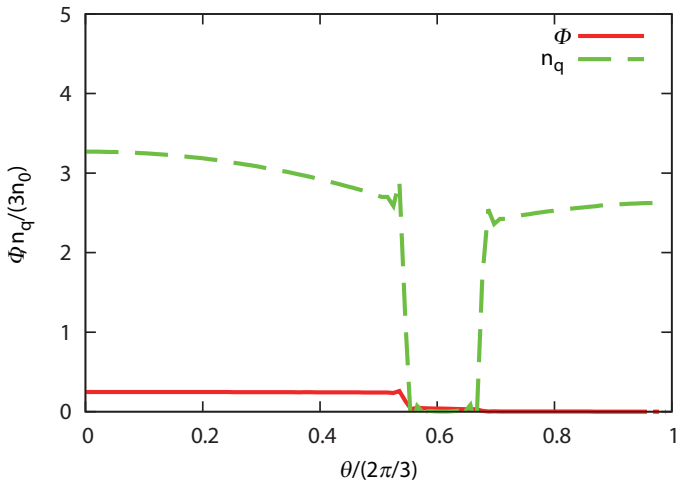


Fig. 8: θ dependence of Φ and the quark number density n_q at $(\mu, T) = (300\ \mathrm{MeV}, 100\ \mathrm{MeV})$ in the PNJL model. See Fig. 7 for the definition of lines.

form of the quark spectrum E_j is not known, we must use numerical differentiation to determine the quark number density n_q, when $\Delta_l \neq 0$. We found that it is very difficult to perform such differentiation with high accuracy in the low temperature region where $T \leq 100$MeV. Then, we adopt the assumption mentioned above and performed the approximated calculations. This assumption is very natural for $\mu = 260$MeV where the chiral symmetry is broken due to large quark mass M but may not be valid for $\mu = 300$MeV where M is small. If the diquark condensate appears at some value of θ in the case of $(\mu, T) = (300\mathrm{MeV}, 100\mathrm{MeV})$, n_q and Φ is not analytic there. Hence, the conclusion that the Taylor-expansion approach of (31) does not work at $(\mu, T) = (300\mathrm{MeV}, 100\mathrm{MeV})$ is not changed.

VI. SUMMARY

In summary, we investigate QCD at large μ/T by using the $SU(3)$ gauge theory with the flavor-dependent twist boundary condition (FTBC). The theory agrees with QCD at $\theta = 0$ and becomes Z_3 symmetric at $\theta = 2\pi/3$. In Z_3-QCD, one can make clear discussion on the relation between Z_3-symmetry and diquark and chiral condensates.

In Z_3-QCD, there can exist a perfectly confined phase where $\Phi = 0$. Since the diquark condensate Δ is an order parameter for both Z_3 symmetry and CSC, Δ is finite (zero) when Φ is finite (zero). The perfectly confined phase with $\Phi = 0$ thus never coexists with the CSC phase with $\Delta \neq 0$. Meanwhile, the chiral condensate as an order parameter for the chiral transition is Z_3 invariant. Hence the chiral transition can take place in the perfectly confined phase.

The phase diagram was numerically investigated for Z_3-QCD with the PNJL model. The perfectly confined phase with $\Phi = 0$ and $\Delta = 0$ appears at $T \lesssim 200$ MeV, and the chiral restoration occurs at $\mu \approx 300$ MeV in the phase. Hence, the perfectly confined phase is divided into the perfectly confined phase without chiral symmetry restoration in a region of $\mu \lesssim 300$ MeV and $T \lesssim 200$ MeV and the perfectly confined phase with chiral symmetry restoration in a region of $\mu \gtrsim 300$ MeV and $100 \lesssim T \lesssim 200$ MeV. In a region of $\mu \gtrsim 300$ MeV and $T \lesssim 100$ MeV, CSC phases with finite Δ and small Φ appear, since they are more stable than the perfectly confined phase with chiral symmetry restoration. This basic structure remains in QCD, although the phase structure is much more complicated in Z_3-QCD than that in QCD. The phase diagram for QCD is thus a remnant of that for Z_3-QCD.

We also showed that in the perfectly confined phase the sign problem may become less serious because of $\Phi = 0$, using the heavy quark model. This may make LQCD simulations feasible in the perfectly confined phase. Particularly when the system is in the perfectly confined phase without chiral symmetry restoration, the system changes continuously from Z_3-QCD to QCD by varying θ from $2\pi/3$ to 0. Using this property, we proposed the Taylor-expansion method of (31) to estimate observables for QCD from those for Z_3-QCD. In the perfectly confined phase with chiral symmetry restoration, however, the system does not change smoothly as θ varies from $2\pi/3$ to 0. Therefore, the lattice QCD framework proposed above may not work. Further study is necessary for this region.

In this paper, we considered three degenerate flavor QCD as the first step. Even in the 2+1 flavor case, there exists a point of $\Phi = 0$ in μ–T plane for some θ near $2\pi/3$ [35]. For example, in the case of infinite m_s (the two-flavor case), such a point appears at $\theta \sim \pi/2$. Hence, we can expect that the present Taylor expansion method is applicable for realistic 2+1 flavor QCD.

Acknowledgments

The authors are thankful especially to I.-O. Stamatescu for useful information on their analyses based on the heavy quark model for finite density and to Y. Sakai and T. Sasaki for many fruitful discussions on the FTBC model. They also thank A. Nakamura, Y. Taniguchi, T. Saito, E.Ito, K. Nagata, R. Fukuda and A. Suzuki for variable comments. H.K. also thanks M. Imachi, H. Yoneyama, H. Aoki, M. Tachibana and T. Makiyama for useful discussions. Four of the authors (H. K., K. K., J. T. and M. Y.) are supported by Grant-in-Aid for Scientific Research (No.26400279, No. 26-1717, No. 25-3944 and No.26400278) from Japan Society for the Promotion of Science (JSPS). The numerical calculations were partially performed by using SX-ACE at CMC, Osaka University.

[1] Z. Fodor, and S. D. Katz, Phys. Lett. B **534**, 87 (2002).
[2] C. R. Allton, S. Ejiri, S. J. Hands, O. Kaczmarek, F. Karsch, E. Laermann, Ch. Schmidt, and L. Scorzato, Phys. Rev. D **66**, 074507 (2002).
[3] S. Ejiri et al., Phys. Rev. D **82**, 014508 (2010).
[4] P. de Forcrand and O. Philipsen, Nucl. Phys. **B642**, 290 (2002).
[5] M. D'Elia and M. P. Lombardo, Phys. Rev. D **67**, 014505 (2003).
[6] M. D'Elia and F. Sanfilippo, Phys. Rev. D **80**, 111501 (2009).
[7] P. de Forcrand and O. Philipsen, Phys. Rev. Lett. **105**, 152001 (2010).
[8] K. Nagata and A. Nakamura, Phys. Rev. D **83**, 114507 (2011).
[9] J. Takahashi, K. Nagata, T. Saito, A. Nakamura, T. Sasaki, H. Kouno, and M. Yahiro Phys. Rev. D **88**, 114504 (2013); J. Takahashi, H. Kouno, and M. Yahiro Phys. Rev. D **91**, 014501 (2015).
[10] G. Aarts, Phys. Rev. Lett. **102**, 131601 (2009).
[11] G. Aarts, L. Bongiovanni, E. Seiler, D. Sexty, and I.-O. Stamatescu, Eur. Phys. J. A **49**, 89 (2013).
[12] D. Sexty, Phys. Lett. B **729**, 108 (2014).
[13] J. Greensite, arXiv:1406.4558 [hep-lat] (2014).
[14] G. Aarts, F. Attanasio, B. Jäger, E. Seiler, D. Sexty, and I.-O. Stamatescu, arXiv:1411.2632 [hep-lat](2014).
[15] M. Cristoforetti et al., Phys. Rev. D **86**, 074506 (2012).
[16] H. Fujii, D. Honda, M. Kato, Y. Kikukawa, S. Komatsu and T. Sano, JHEP **1310**, 147 (2013).
[17] P. N. Meisinger, and M. C. Ogilvie, Phys. Lett. B **379**, 163 (1996).
[18] A. Dumitru, and R. D. Pisarski, Phys. Rev. D **66**, 096003 (2002); A. Dumitru, Y. Hatta, J. Lenaghan, K. Orginos, and R. D. Pisarski, Phys. Rev. D **70**, 034511 (2004); A. Dumitru, R. D. Pisarski, and D. Zschiesche, Phys. Rev. D **72**, 065008 (2005).
[19] K. Fukushima, Phys. Lett. B **591**, 277 (2004)..
[20] C. Ratti, M. A. Thaler, and W. Weise, Phys. Rev. D **73**, 014019 (2006); C. Ratti, S. Rößner, M. A. Thaler, and W. Weise, Eur. Phys. J. C **49**, 213 (2007).
[21] E. Megias, E. Ruiz Arriola, and L. L. Salcedo, Phys. Rev. D **74**, 065005 (2006).
[22] S. Rößner, C. Ratti, and W. Weise, Phys. Rev. D **75**, 034007 (2007).
[23] B. -J. Schaefer, J. M. Pawlowski, and J. Wambach, Phys. Rev. D **76**, 074023 (2007).
[24] H. Abuki, R. Anglani, R. Gatto, G. Nardulli, and M. Ruggieri, Phys. Rev. D **78**, 034034 (2008).
[25] K. Fukushima, Phys. Rev. D **77**, 114028 (2008).
[26] K. Kashiwa, H. Kouno, M. Matsuzaki, and M. Yahiro, Phys. Lett. B **662**, 26 (2008).
[27] Y. Sakai, K. Kashiwa, H. Kouno, and M. Yahiro, Phys. Rev. D **77**, 051901 (2008); Phys. Rev. D **78**, 036001 (2008).
[28] L. McLerran K. Redlich and C. Sasaki, Nucl. Phys. A **824**, 86 (2009).
[29] T. Sasaki, Y. Sakai, H. Kouno, and M. Yahiro, Phys. Rev. D **84**, 091901 (2011).
[30] A. M. Polyakov, Phys. Lett. **72B**, 477 (1978).
[31] Y. Aoki, G. Endrödi, Z. Fodor, S. D. Katz and K. K. Szabó, Nature **443**, 675 (2006).
[32] H. Kouno, Y. Sakai, T. Makiyama, K. Tokunaga, T. Sasaki, and M. Yahiro, J. Phys. G: Nucl. Part. Phys. **39**, 085010 (2012).
[33] Y. Sakai, H. Kouno, T. Sasaki, and M. Yahiro, Phys. Lett. B **718**, 130 (2012).
[34] H. Kouno, K. Kashiwa, T. Misumi, T. Makiyama, T. Sasaki, and M. Yahiro, Phys. Rev. D **88**, 016002 (2013).
[35] H. Kouno, T. Makiyama, T. Sasaki, Y. Sakai, and M. Yahiro, J. Phys. G: Nucl. Part. Phys. **40**, 095003 (2013).
[36] S. Borsanyi, Z. Fodor, C. Hoelbling, S.D. Katz, S. Krieg, C. Ratti, K. K. Szabo, JHEP **1009:073** (2010).
[37] A. Bazavov et al., Phys. Rev. D**85**, 054503 (2012). JHEP **1009:073** (2010).
[38] A. Roberge and N. Weiss, Nucl. Phys. **B275**, 734 (1986).
[39] G. Boyd, J. Engels, F. Karsch, E. Laermann, C. Legeland, M. Lütgemeier, and B. Petersson, Nucl. Phys. **B469**, 419 (1996).
[40] O. Kaczmarek, F. Karsch, P. Petreczky, and F. Zantow, Phys. Lett. B **543**, 41 (2002).
[41] S. Borsányi, Z. Fodor, C. Hoelbling, S. D. Katz, S. Krieg, C. Ratti, and K. K. Szabo, arXiv:1005.3508 [hep-lat] (2010).
[42] W. Söldner, arXiv:1012.4484 [hep-lat] (2010).
[43] K. Kanaya, arXiv:hep-ph/1012.4235 [hep-ph] (2010); arXiv:hep-ph/1012.4247 [hep-lat] (2010).
[44] S. B. Rüster, V. Werth, M. Buballa, I. A. Shovkovy, and D. H. Rischke, Phys. Rev. D **72**, 034004 (2005).
[45] M. Kobayashi, and T. Maskawa, Prog. Theor. Phys. **44**, 1422 (1970); M. Kobayashi, H. Kondo, and T. Maskawa, Prog. Theor. Phys. **45**, 1955 (1971).
[46] G. 't Hooft, Phys. Rev. Lett. **37**, 8 (1976); Phys. Rev. D **14**, 3432 (1976); **18**, 2199(E) (1978).
[47] P. Rehberg, S.P. Klevansky and J. Hüfner, Phys. Rev. C **53**, 410 (1996).